EarlyType Galaxies: Data

Presentation

by

Ytsen Haringa

Outline

- Early-type galaxies in the present
- The fundamental plane of early-type galaxies
- Evolution of early-type galaxies
- Balmer absorption line strength evolution
- Progenitor bias

Early-type galaxies in the present

- Mostly pop II stars, some old pop I stars
- Low dust content
- Dominated by random motion
- Vary in mass, size and luminosity
- “Dynamically hot”

Fundamental plane

- $I \sim V^2/GR(M/L)$ Virial theorem
- Central velocity dispersion
- Effective radius
- Effective surface brightness

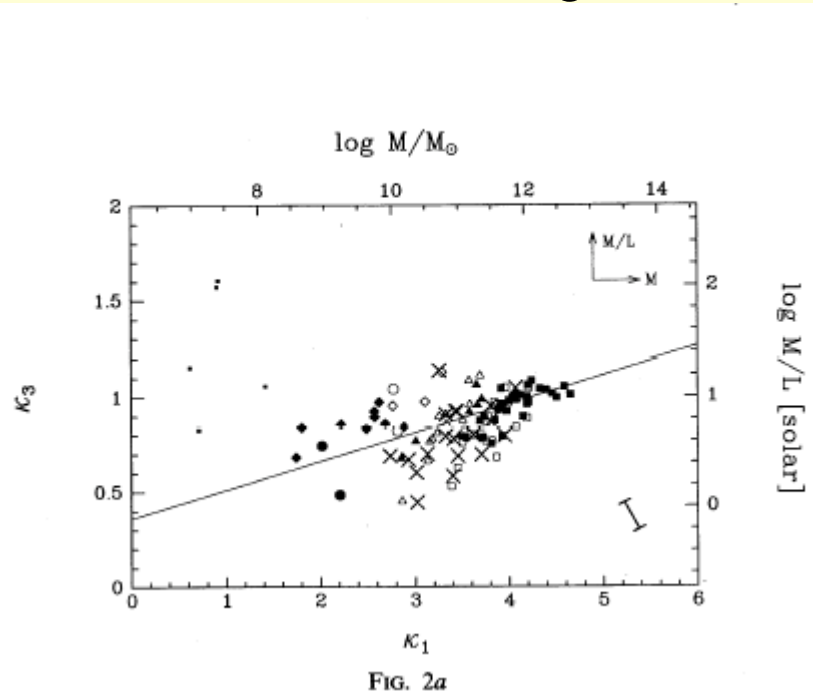

FIG. 2a

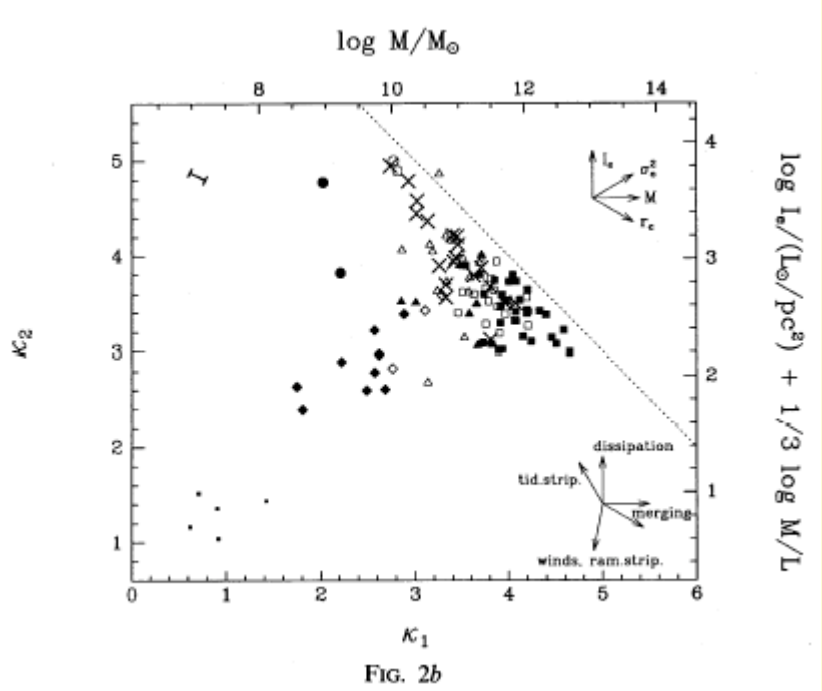

FIG. 2b

Evolution of early-type galaxies

- Tilt of the FP
- Mass dependence

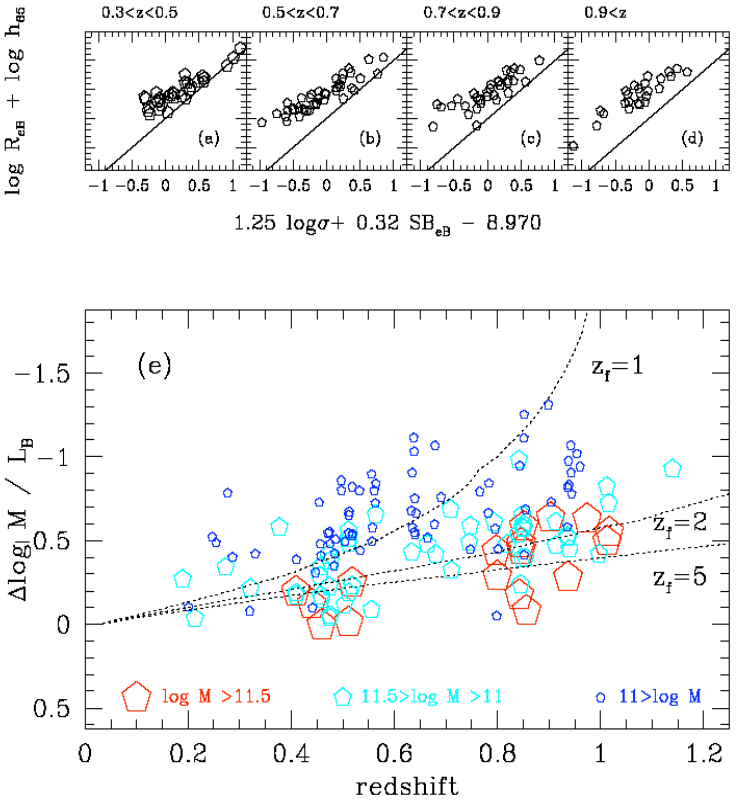

Fig. 1.— Top panels: edge-on view of the FP in redshift bins. The solid line represents the FP for the Coma cluster. Bottom panel: offset from the Coma FP, coded by dynamical mass demonstrating the stronger evolution for smaller masses. Typical errors are < 0.1 dex on the vertical axis. Dotted lines represent passive evolutionary trends for single burst models at various formation epochs (z_f).

Frosting model

- Z-plane
- Metallicity
- Time
- Velocity dispersion

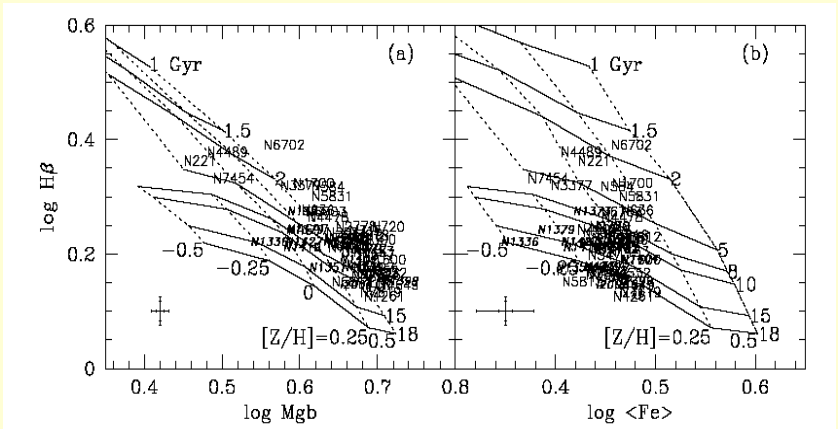

FIG. 1.—Line strengths of G93 (*roman type, smaller error bars*) and Fornax ellipticals (*slanted bold type, larger error bars*) through the central $r_e/8$ aperture. Solar-ratio model grids from Worthey (1994) have been superposed: solid lines are contours of constant age (from top, 1, 1.5, 2, 5, 8, 10, 15, 18 Gyr), and dotted lines are contours of constant [Z/H] (*from left*, [Z/H] = −0.5, −0.25, 0.0, +0.25, +0.5 dex, except at ages younger than 8 Gyr, where from left [Z/H] = −0.225, 0.0, +0.25, +0.5 dex). (*a*) Mg *b* and Hβ line strengths. (*b*) ⟨Fe⟩ and Hβ line strengths. Differences in the ages and metallicities inferred from the two diagrams result from the nonsolar abundance ratios of giant elliptical galaxies. Our procedure corrects for this and in so doing derives the nonsolar abundance ratio, [E/Fe].

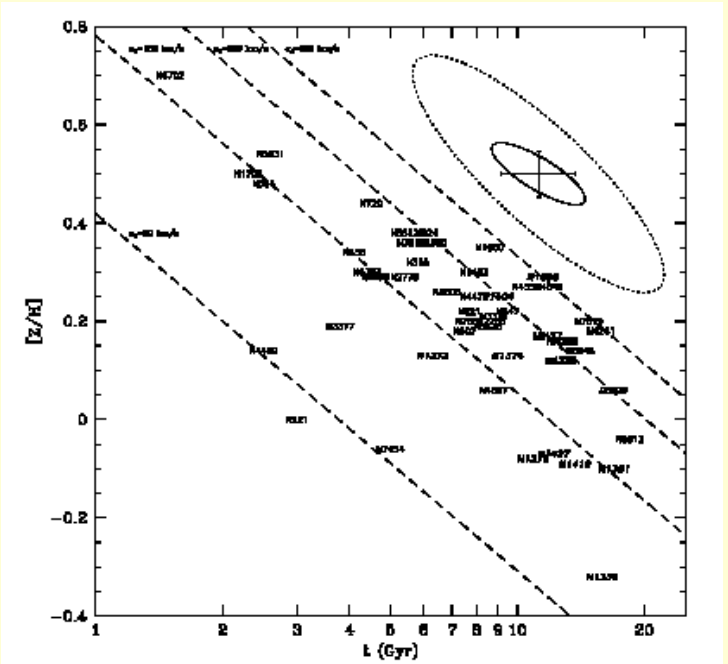

FIG. 4.—Face-on view of the Z-plane in hyperspace (*points as in Fig. 1*). At fixed velocity dispersion (*dashed lines*), younger galaxies have higher metallicities than older galaxies. The solid error ellipse in the top right-hand corner is typical of the G93 sample; the dotted ellipse is typical of the highest quality data in the Lick/IDS galaxy sample (TWFBG98). The slope of the error ellipses is nearly identical to the of lines of constant velocity dispersion, indicating that poor data can masquerade as real trends.

Single star burst scenario

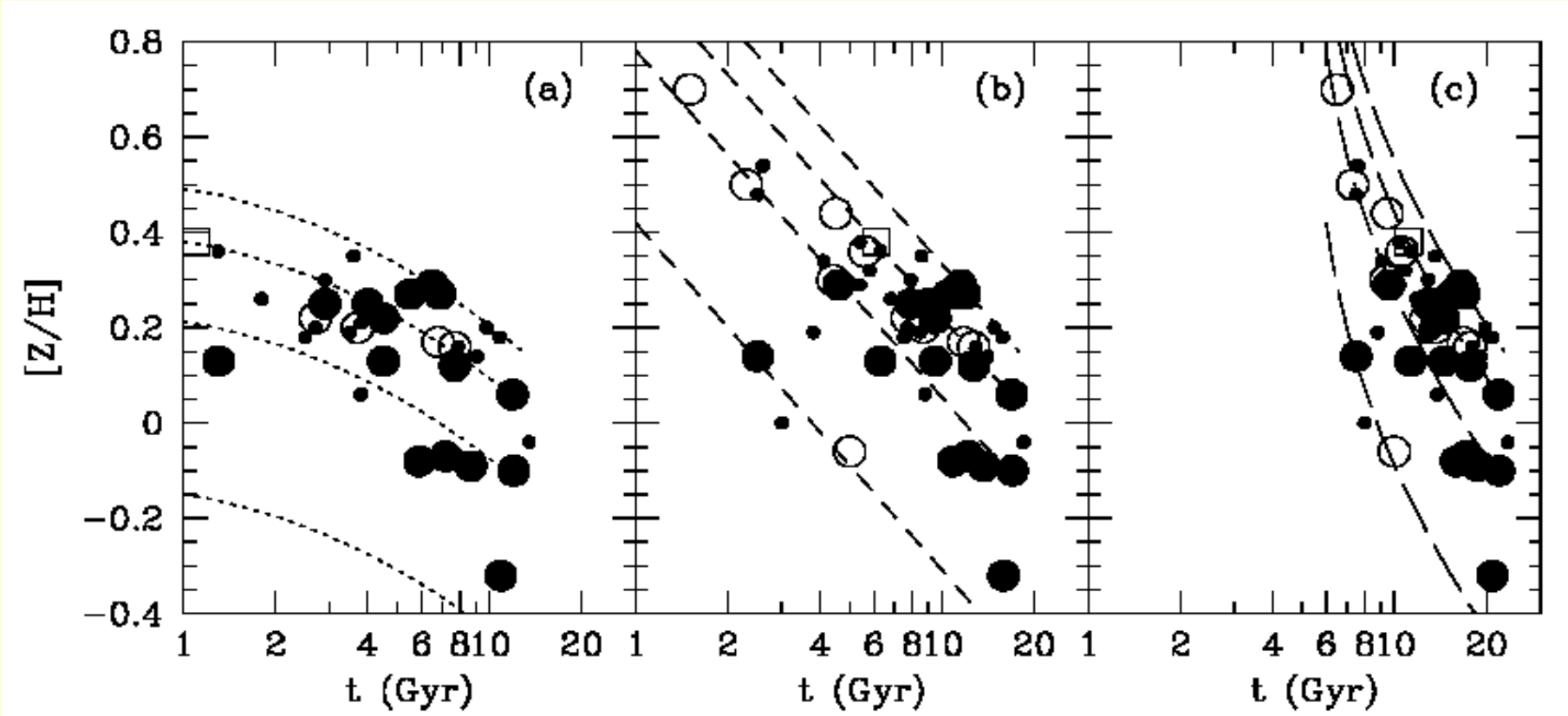

FIG. 10.—Time evolution of galaxies in the Z-plane for pure SSPs. Points are coded by environment (see Fig. 7). Lines are loci of constant velocity dispersion: from bottom to top, $\sigma_0 = 50$, 150, 250, 350 km s^{-1} (see Fig. 4). (*a*) Metallicity hyperplane 5 Gyr ago. (*b*) Metallicity hyperplane today. (*c*) Metallicity hyperplane 5 Gyr from now. Note the strong curvature in lines of constant σ in panels (*a*) and (*c*).

Double star burst scenario

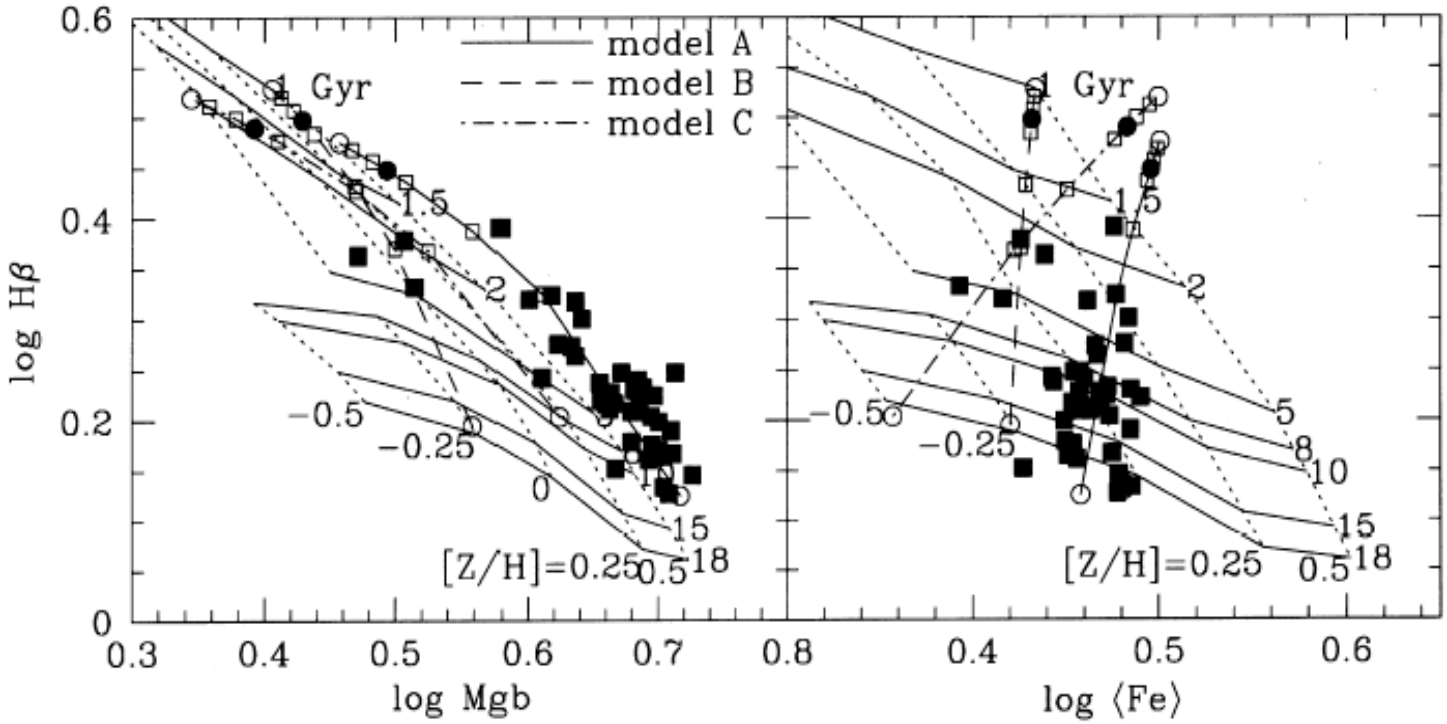

FIG. 12.—Schematic two-burst models. Three models are shown: (*a*) 17 Gyr, [Z/H] = +0.15 dex, [E/Fe] = +0.25 dex progenitor (typical of the oldest giant ellipticals in the sample) with a 1 Gyr, [Z/H] = +0.75 dex, solar-neighborhood abundance ratio burst, meant to cover the stellar populations of the high-σ galaxies (*solid line*); (*b*) 17 Gyr, [Z/H] = −0.25 dex, solar-neighborhood abundance ratio progenitor with a 1 Gyr, [Z/H] = +0.5 dex, solar-neighborhood abundance ratio burst, meant to cover the stellar populations of the low-σ galaxies NGC 221 (M32), NGC 4489, and NGC 7454 (*short-dashed line*); and (C) a 17 Gyr, [Z/H] = −0.25 dex, [E/Fe] = +0.25 dex progenitor with a 1 Gyr, [Z/H] = +0.5 dex, [E/Fe] = −0.25 burst dex, meant to represent possible star formation after a metal-enriched wind in a low-σ galaxy (*dot-dashed line*). Bursts of 10%, 20%, 40%, 60%, and 80% (*open squares*) and 50% (*filled circles*) by mass are shown. Open circles represent the progenitor (*lower*) and burst (*upper*) populations. Filled squares are the G93 galaxies; compare with Fig. 1.

Balmer line absorption

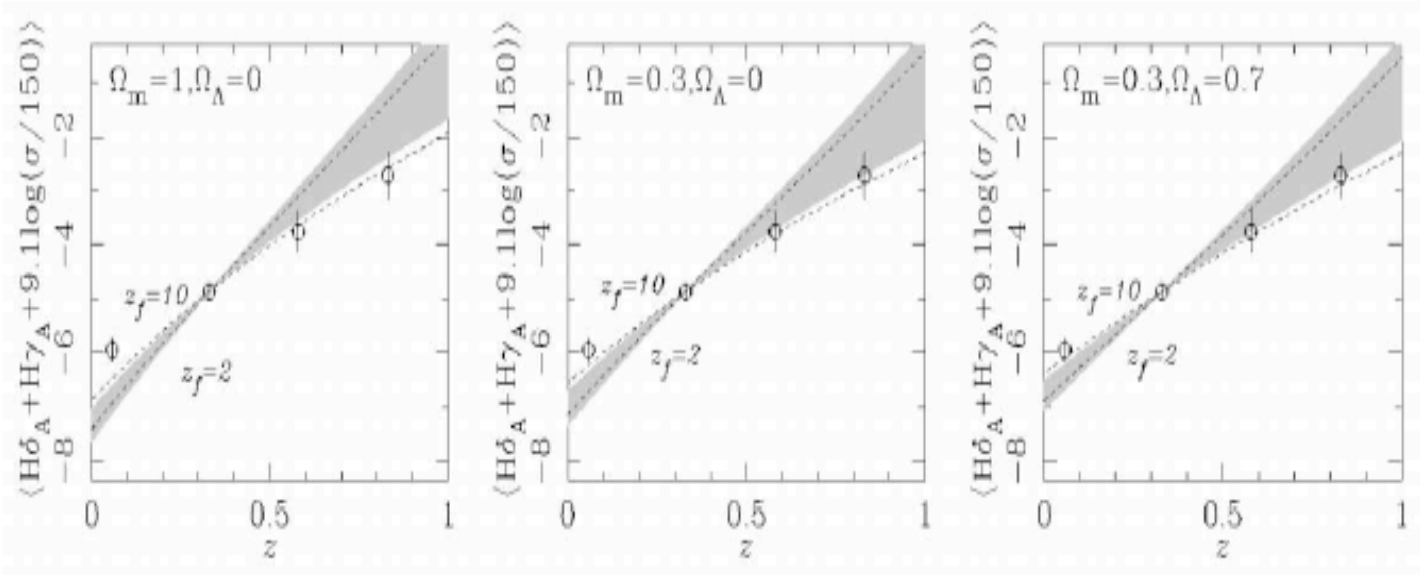

FIG. 3.—The $(H\delta_A + H\gamma_A)$–σ zero-point evolution as a function of redshift, with single-burst stellar population models of Vazdekis et al. (1996; *dashed lines*) and Worthey (1994; Trager et al. 2000; *shaded regions*). The model curves, shown for formation epochs of $2 \le z_f \le 10$, are insensitive to the shape of the IMF. Together, the data and models provide lower 95% confidence limits for the mean epoch of star formation of $z_f > 2.9$ and $z_f > 2.4$ using the Worthey and Vazdekis et al. models, respectively, for $\Omega_m = 0.3$ and $\Omega_\Lambda = 0.7$.

Progenitor bias

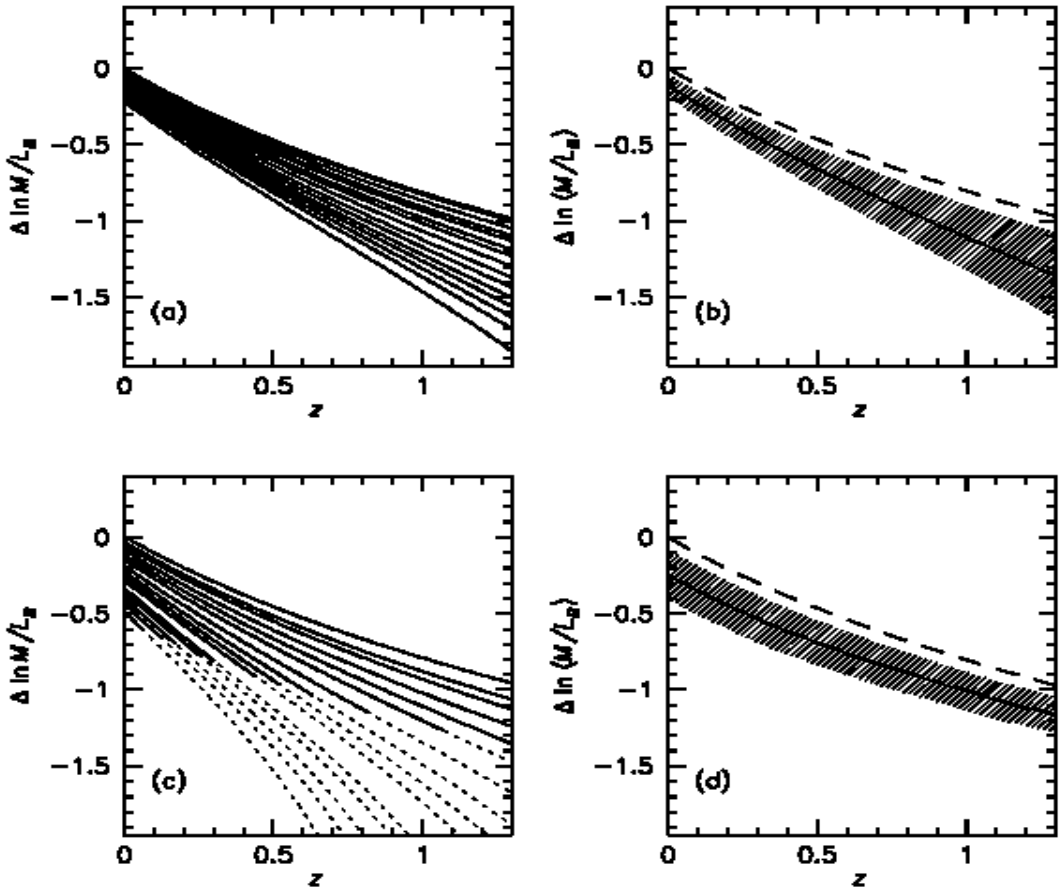

FIG. 1.—Illustration of the evolution of early-type galaxies in traditional models (*a and b*) and in models with morphological evolution (*c and d*). Lines in (*a*) and (*c*) show the evolution of individual galaxies with a range of ages. The dashed sections of the curves in (*c*) indicate that the galaxies are not yet recognized as early-type galaxies. Panels (*b*) and (*d*) show the evolution of the mean M/L ratio in these two models. The scatter is indicated by the width of the hatched regions. The dashed line shows the evolution of a single-age stellar population formed at $z = \infty$. In models with morphological evolution, the mean M/L ratio evolves slowly and the scatter is roughly constant because more and more young galaxies drop out of the sample at high redshift.

References

- **Kelson et al.** Evolution of early-type galaxies in distant clusters: the fundamental plane from Hubble Space Telescope imaging and Keck spectroscopy
- **Bender, Burnstein & Faber** Dynamically hot galaxies. I. structural properties
- **Van Dokkum & Franx** Morphological evolution and the ages of early-type galaxies in clusters
- **Treu et al.** Keck spectroscopy of distant GOODS spheroidal galaxies: downsizing in a hierarchical universe
- **Trager et al.** The stellar population histories of early-type galaxies. II. controlling parameters of the stellar populations
- **Kelson et al.** The evolution of balmer absorption line strengths in E/S0 galaxies from $z = 0$ to $z = 0.83$